International Journal of Industrial Electronics, Control and Optimization © 2021 IECO
Vol. 4, No.3, pp. 341-353, July (2021)

Dynamic Stability Improvement of Power System with Simultaneous and Coordinated Control of DFIG and UPFC using LMI

Masoud Maleki Rizi[1], Saeed Abazari[2†], Nima Mahdian[3]

[1,2]Department of Engineering, University of Shahrekord, Shahrekord, Iran
[3] Shahid Rajaee Teacher training University, Tehran, Iran.

ABSTRACT

This paper presents an enhancement of the dynamic stability of a power system equipped with both a unified power flow controller (UPFC) and a doubly-fed induction generator (DFIG) by using the LMI technique. We use all UPFC main basic PI controllers and its power oscillation damping (POD) supplementary controller. A more complete model of DFIG and both rotor-side converter (RSC) and grid-side converter (GSC) dynamics with their controllers are considered, too. These two devices controllers are simultaneously coordinated and optimized with compromising between their control variables parameters. The particle swarm optimization (PSO) algorithm is used to optimize the objective function based on eigenvalues and damping ratio to reach the best parameters and variables of controllers of both UPFC and DFIG. Linear matrix inequality (LMI) is applied to the whole system linearized model to reach optimally modified eigenvalues. Within the steady state and dynamic study, we consider practical line thermal capacity and UPFC power rating, too. Simulation results in 39-bus 10-machine New-England power systems illustrate the capability of the applied method. The results demonstrate that coordinated control of these two devices besides using LMI results in more damping of system modes oscillations and more stability in the power system.

Article Info

Keywords:
Dynamic stability, Doubly-fed induction generator, Linear Matrix Inequality, Optimization, Unified power flow controller.

Article History:
Received 2021-02-12
Accepted 2021-06-01

I. INTRODUCTION

The unified power flow controller (UPFC) is an effective flexible alternating current transmission system (FACTS) device that helps overcome some of existing power system operation limitations. It is the most important and comprehensive device that helps stability improvement in power systems. UPFC is equipped with a power oscillation damping (POD), and the damping effect of this POD is better than the power system stabilizer (PSS).

On the other hand, wind energy conversion systems (WECS) are growing fast due to environmental issues and the limitations of natural resources. The application of wind energy to produce electrical energy using doubly-fed induction generators (DFIGs) is growing in power systems because DFIGs allow a larger portion of the wind energy to be absorbed. The interaction of DFIG controllers will occur with both electrical and mechanical system modes leading to electrical and mechanical oscillations [1]. Then, the effect of these devices on power system oscillations and stability is an important issue.

The stability enhancement of a three-machine system by using the coordinated application of the UPFC and the PSS designed employing the Firefly algorithm was already

[†]**Corresponding Author:** abazari-s@eng.sku.ac.ir
Tel: +98-9133144539, Faculty of Electrical Engineering, Shahrekord University, Shahrekord, Iran.

compared with the genetic search algorithm approach [2]. To UPFC POD controller design in MMPS, in three-machine system, with selecting damping ratio based objective function LQR (Linear Quadratic Regulation) have used under different loading condition and better result demonstrated [3]. The improved grey wolf optimizer (IGWO) was compared with differential evolution (DE) and particle swarm optimization(PSO) to optimize UPFC POD controller with integral of time-weighted absolute error (ITAE) criteria too and the results demonstrated the stability enhancement of MMPS in the three-machine system while comparing using either m_B or δ_E [4].

On the other hand, the effect of DFIG controllers and system parameters in linear modal analysis of DFIG torsional interaction was investigated and the results showed that the DFIG controllers should be adjusted, otherwise, an interaction may occur and the system oscillations may increase, which may even make the system unstable. The damping mechanisms of power systems were analytically compared with induction generator-based wind power generation by Bu in a multi-machine power system in which a model with rotor-side converter (RSC) dynamics and a model without RSC dynamics with fixed rotor speed and with offset rotor voltage only and with constant rotor voltage were investigated [5].

Today, power systems may consist of both of these two important devices because of their operational, economic, and environmental advantages. Beside these advantages, they have interactions and influence the stability of power systems. So, many studies have recently focused on the effects of each of these two devices on the other device or the overall power system.

UPFC can be used to improve the overall performance of WECS through the development of an appropriate control algorithm. The application of a UPFC control algorithm is also investigated in one research to overcome some problems associated with the internal faults associated with WECS [6]. Based on power control and speed error minimization objectives, wind turbines were utilized in a research study,and to improve reactive and real power, IEEE-9 and 14 bus systems were investigated by installing UPFC in the transmission line. [7]. The simulation results show that UPFC can improve the low voltage ride-through (LVRT) of DFIG-based WECS, reduce machine oscillations, and finally maintain wind turbine connection to the grid during certain levels of voltage fluctuations on the grid side and fault conditions [8]-[10]. UPFC can noticeably improve the fault ride-through (FRT) capability of WECS, so it can support the grid during fault conditions [11]. UPFC has been used in a DFIG-based wind turbine system to provide dynamic reactive power support at the PCC in the occurrence of three-phase fault conditions [12]. In a transient stability study, a control proposed for the admittance model of the UPFC was validated in a DFIG wind farm penetrated power system. The power output of the DFIG was stabilized, which helped recover rotor angular deviation of the respective generators, which significantly stabilized the network [13]. Performance of wind power and UPFC to increase the fault critical clearing time of power system using MATLAB/SIMULINK software simulated the IEEE 3 machines 9 buses verified and showed that the better result will be obtained while these two devices are in the optimum location [14].

Linear matrix inequality (LMI)-based techniques have already been used for the stability of power systems that are equipped with UPFC to have optimal control while the LMI approach is used for optimal pole placement [15]. This approach has been used in the robust adaptive model predictive control of DFIG [16]. But, it has not been employed in multi- machine power systems consisting of both of these two devices. Then, we applied LMI in order to optimize pole placement more optimally and improve the robustness of this large power system linear system model.

Then, it is important to study and improve this stability in the systems in which both UPFC and DFIG are installed. Here, we have studied more complete small signal models of UPFC and DFIG to investigate the damping effects of UPFC and DFIG in multi-machine power systems considering all dynamic states of both of them in comparison with previous studies. We have considered practical constraints too while using PSO (its detail algorithm can be found in [17]). To optimize the control parameters of each of them, LMI was applied to the system to have optimal eigenvalues, too.

The main contributions of the study are the application of all classic controllers of UPFC together, the application of practical constraints of line and UPFC capacities, the use of DFIG complete electrical model and all of its converters controllers, the use of PSO to optimize simultaneously and coordinated UPFC and DFIG controllers, the use of LMI approach to more optimization in eigenvalues of the whole system, and increasing the whole control system robustness.

The following sections introduce UPFC and its small signal model and control aspects. Then, DFIG small signal modeling and control are reviewed. Then, the combined power system model with UPFC installed and DFIG connected models are presented. PSO algorithm and LMI technique, which have been used, are briefly described too. In the last section, the simulation results of these two devices that are applied to dynamic stability individually and together are demonstrated and compared.

II. UNIFIED POWER FLOW CONTROLLER

As is seen in Figure 1, UPFC consists of two converters coupled through a common DC link. Eq. (1) expresses the UPFC terminals voltages.

$$\bar{V}_E = \frac{m_E V dc}{2} e^{j\delta_E}, \bar{V}_B = \frac{m_B V dc}{2} e^{j\delta_B} \quad (1)$$

Where

m_B is the pulse width modulation index of the series(boosting) inverter, m_E is the pulse width modulation index of the shunt (exciting) inverter, δ_B is the phase angle of the series injected voltage, and δ_E is the voltage phase angle of the shunt inverter.

The series branch of the UPFC injects an AC voltage with controllable magnitude and phase angle at the power frequency. Then, it can exchange real and reactive power with the installed line. The shunt converter is primarily used to provide active power demand of the series converter through a common DC link and can exchange reactive power to adjust the voltage of the bus, which is connected. So, due to these capabilities, UPFC is an excellent choice for damping power system oscillations. This damping can be obtained by regulating the abovementioned controllable parameters by controlling the decoupled variables of the UPFC by the following four controllers:

$$\delta_B = \left(\frac{1}{1+T_{\delta B}S}\right)\left(K_{Pp} + \frac{K_{Pi}}{s}\right)\left(P_{Ref} - P\right) \quad (2)$$

$$m_B = \left(\frac{1}{1+T_{mBS}}\right)\left(K_{Qp} + \frac{K_{Qi}}{s}\right)\left(Q_{Ref} - Q\right) \quad (3)$$

$$m_E = \left(\frac{1}{1+T_{mES}}\right)\left(K_{Vp} + \frac{K_{Vi}}{s}\right)\left(V_{Ref} - V\right) \quad (4)$$

$$\delta_E = \left(\frac{1}{1+T_{\delta ES}}\right)\left(K_{DCp} + \frac{K_{DCi}}{s}\right)\left(V_{DC,Ref} - V_{DC}\right) \quad (5)$$

Where

T_x is delay time constants, and K_{xp} and K_{xi} are PI controllers proportional and integral gains, respectively, P, Q, V and V_{DC} are active and reactive power flow through line and bus voltage to which UPFC is connected and UPFC dc link voltage, respectively.

Comprehensive models of UPFC for steady-state, transient stability and dynamic stability studies and also a dynamic model of the system installed with UPFC are presented in [18] and [19]. A unified model of a multi-machine power system and developed UPFC models is proposed that has been linearized and incorporated into the Heffron-Phillips model [19]. The conflict between UPFC multiple control functions and their interactions was investigated and it was shown that the application of all four control functions may sometimes decrease the accuracy of the results [20]. We used all of these four controllers simultaneously and made a compromise between four control variables. Due to technical and economical restrictions, the rating of the UPFC power is limited and this leads to applying limits of its real and reactive power by additional limiter blocks and then modifying the UPFC related parameters in each of iteration.

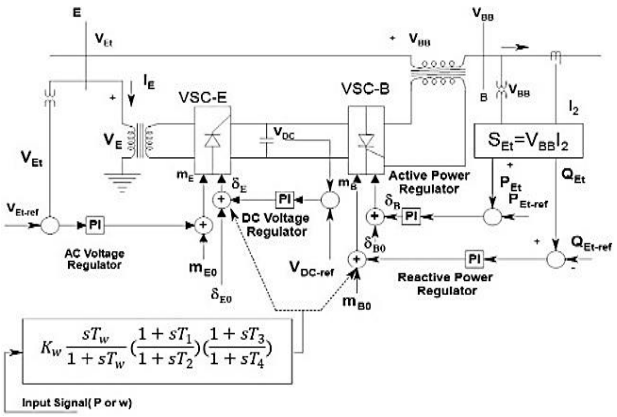


Fig. 1. The UPFC power and control flow diagram

A supplementary controller, known as POD, is designed in UPFC to enhance the transient stability of the entire electric power system. Inverse interaction between PSS and series part control is compensated by providing a UPFC-based damping controller [21]. As shown in Figure 1, POD controllers have a lead-lag controller structure transfer function consisting of gain, a washout function, and two lead-lag blocks, which should be adjusted. Fixed parameter classical controller is not suitable for the UPFC damping control design. Then, a flexible controller should be developed. Several approaches have been proposed for it, such as root locus and sensitivity analysis, pole placement, and robust control. The conventional techniques require heavy computation and have slow convergence. The search methods may also be trapped in a local minimum and the solution obtained may not be the finest. In addition, it is necessary that the designed controller provide some robustness to the variations of parameters, conditions, and configurations. Also, the controller parameters, which have stabilized the system in a certain operating condition, may no longer have acceptable results in case of large disturbances [22].

To improve its dynamic performance, its parameters can be optimized by using an optimization problem. Based on eigenvalues, a multi-objective function related to the damping factor and damping ratio is considered as:

$$J = \sum_{j=1}^{NP}\sum_{\sigma_i \geq \sigma_0}\left(\sigma_0 - \sigma_{ij}\right)^2 + \alpha\sum_{j=1}^{NP}\sum_{\zeta_i \geq \zeta_0}\left(\zeta_0 - \zeta_{ij}\right)^2$$

$$f(x) = \min J \quad (6)$$

$$K^{\min} \leq K \leq K^{\max}$$

$$T_1^{\min} \leq T_1 \leq T_1^{\max}$$

$$T_2^{\min} \leq T_2 \leq T_2^{\max}$$

$$T_3^{\min} \leq T_3 \leq T_3^{\max}$$

$$T_4^{\min} \leq T_4 \leq T_4^{\max}$$

Where σ_{ij} is the real parts of system eigenvalues, σ_0 is

desired real part of eigenvalue, ζ_{ij} is the damping ratios of system variables, and ζ_0 is the desired damping ratio. This optimization problem can use a numerical technique, such as PSO.

III. An Introduction to DFIG Study

In DFIG, two converters are included in the rotor circuit. The power electronic converters ratio is a fraction of the total power. Therefore, the losses in the power electronic converter can be reduced compared to a system where the converter has to handle the entire power, and the system cost is lower due to the partially rated power electronics. DFIG operates in both sub-synchronous and super-synchronous modes with a rotor speed range around the synchronous speed. For variable-speed systems, DFIG offers adequate performance [23]. Figure 2 shows a DFIG-based wind farm connected to a power system.

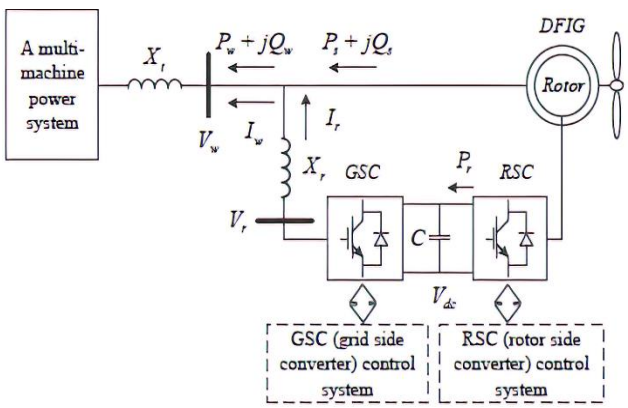


Fig. 2. DFIG connected to a multi-machine power system

In [24], different state space models of DFIG for power system study have been compared. The modeling details of the turbine, drive train**,** pitch controller, induction machine, and the controllers of both RSC and the grid-side converter (GSC) of DFIG have been introduced.

DFIG state equations in dynamic stability studies are mentioned below.

Eq. (7)-(10) are related to two-mass model turbine drive dynamic, Eq. (11)-(13) are for the three-degree model of the machine, Eq. (14)-(17) are related to for GSC controller, and Eq. (18)-(21) are for RSC controller as follows:

$$2H_t \frac{d\omega_t}{dt} = T_m - T_{sh} \quad (7)$$

$$2H_g \frac{d\omega_g}{dt} = T_{sh} - T_e \quad (8)$$

$$\frac{1}{\omega_b}\frac{d\theta_{tw}}{dt} = \omega_t - \omega_g \quad (9)$$

$$T_{sh} = D\frac{d\theta_{tw}}{dt} + K\theta_{tw} \quad (10)$$

$$T_0' \frac{dE'_{qD}}{dt} = -\left(E'_{qD} + (X_s - X_s')I_{ds}\right) + T_0'\left(\omega_s \frac{X_m}{X_r} V_{dr} - (\omega_s - \omega_r)E'_{dD}\right) \quad (11)$$

$$T_0' \frac{dE'_{dD}}{dt} = -\left(E'_{dD} + (X_s - X_s')I_{qs}\right) + T_0'\left(\omega_s \frac{X_m}{X_r} V_{qr} - (\omega_s - \omega_r)E'_{qD}\right) \quad (12)$$

$$2\frac{H_D}{\omega_s}\frac{d\omega_r}{dt} = T_m - E'_{dD}I_{ds} - E'_{qD}I_{qs} \quad (13)$$

While:

$$V_{qs} = -R_s I_{qs} - X_s' I_{ds} + E'_{qD}$$

$$V_{ds} = -R_s I_{ds} + X_s' I_{qs} + E'_{dD}$$

$$I_{dr} = \frac{E'_{qD}}{X_m} + \frac{X_m}{X_r} I_{ds} \quad , \quad I_{qr} = -\frac{E'_{dD}}{X_m} + \frac{X_m}{X_r} I_{qs}$$

$$T_0' = \frac{X_r}{\omega_s R_r} \quad , \quad X_s' = X_s - \frac{X_m^2}{X_r}$$

$$E'_{qD} = \frac{X_m}{X_r}\varphi_{qr} \quad , \quad E'_{dD} = -\frac{X_m}{X_r}\varphi_{qr}$$

Considering RSC and GSC dynamic via defining auxiliary variables, x_1 to x_8, which are displayed in Figure 3, are as follows:

$$dx_1 = \frac{1}{K_{I1}}(\omega_{ref} - \omega_r) \quad (14)$$

$$dx_2 = \frac{1}{K_{I2}}(i_{qr} - (-x_1 + K_{P1}((\omega_{ref} - \omega_r)))) \quad (15)$$

$$dx_3 = \frac{1}{K_{I3}}(Q_{sref} - Q_s) \quad (16)$$

$$dx_4 = \frac{1}{K_{I4}}(i_{dr} - (-x_3 + K_{P3}((Q_{sref} - Q_s)))) \quad (17)$$

$$dx_5 = \frac{1}{K_{I5}}(V_{DCref} - V_{DC}) \quad (18)$$

$$dx_6 = \frac{1}{K_{I6}}(i_{qg} - (-x_5 + K_{P5}((V_{DCref} - V_{DC})))) \quad (19)$$

$$dx_7 = \frac{1}{K_{I7}}(V_s - V_{sref}) \quad (20)$$

$$dx_8 = \frac{1}{K_{I8}}(i_{dg} - (-x_7 + K_{P7}((V_s - V_{sref})))) \quad (21)$$

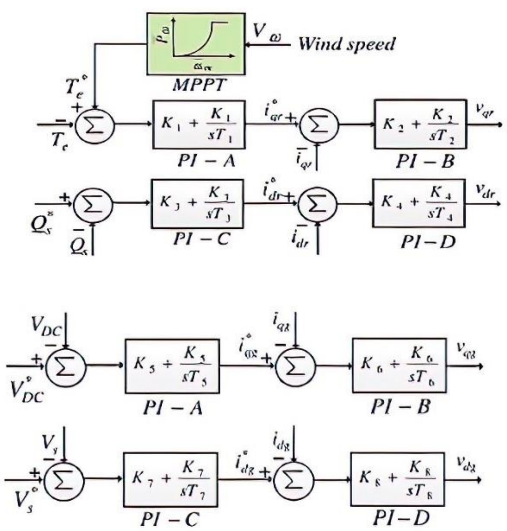


Fig. 3. DFIG RSC and GCS PI controllers

The equation, which represents DC link capacitor between two converters dynamic, is as follows:

$$C_D V_{DC} \frac{dV_{DC}}{dt} = \left(v_{dr} i_{dr} + v_{qr} i_{qr}\right) - \left(v_{dg} i_{dg} + v_{qg} i_{qg}\right) \quad (22)$$

IV. Modeling Power System with UPFC Installed

The performance analysis of UPFC requires its steady-state and dynamic models. Figure 4 shows UPFC in a multi-machine power system:

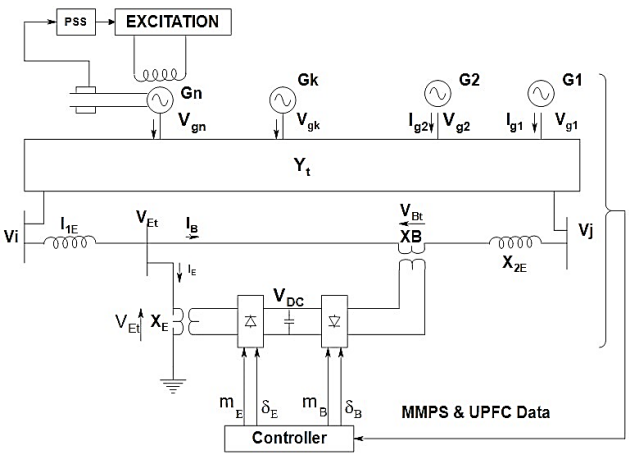


Fig. 4. UPFC in the multi-machine power system

With reducing the bus admittance matrices to generator internal buses and UPFC terminal buses, the following equation can be written:

$$\overline{YE} = \bar{I}\ ,\ \overline{Y} = \begin{bmatrix} Y_{GG} & Y_{GU} \\ Y_{UG} & Y_{UU} \end{bmatrix},\ \overline{E} = \begin{bmatrix} \overline{E}_G \\ \overline{V}_U \end{bmatrix},\ \bar{I} = \begin{bmatrix} \bar{I}_G \\ \bar{I}_U \end{bmatrix} \quad (23)$$

While Y_{GG} is the reduced admittance matrices connecting the generator current injection to the internal generator voltages. Y_{GU} is the admittance matric component, which gives the generator currents due to the voltages at UPFC buses, Y_{UG} is the admittance matrices component, which gives UPFC currents in terms of the generator internal voltages, Y_{UU} is the admittance matrices connecting UPFC currents to the voltages at UPFC buses, $\overline{E}_G$ is the vector of generator internal bus voltages, $\overline{V}_U$ is the vector of UPFC ac bus voltages, $\bar{I}_G$ is the vector of generators' currents injection, $\bar{I}_U$ is the vector of UPFC currents injected to the power network. Then these parameters values will incorporate in deriving matrices equation of multi machine power system with UPFC installed which is essential in dynamic stability analysis.

For the small signal stability studies of the power system, the linear model of Heffron-Phillips is used, which provides reliable and enough accurate results [25]. The nonlinear dynamic model of the system installed with the UPFC equations is as follows:

$$\dot{\delta} = \omega_b(\omega - 1) \quad (24)$$

$$\dot{\omega} = M^{-1}\left(T_m - T_e - D(\omega - 1)\right) \quad (25)$$

$$\dot{E}'_q = T'_{do}\left(E_{fd} - E'_q + (X_d - X'_d)I_d\right) \quad (26)$$

$$\dot{E}_{fd} = \left(K_A\left(V_{Ref} - V_t\right) - E_{fd}\right)/T_A \quad (27)$$

$$\dot{V}_{DC} = \frac{3m_E}{4C_{dc}}\left(sin\delta_E I_{Ed} + cos\delta_E I_{Eq}\right) + \frac{3m_B}{4C_{dc}}\left(sin\delta_B I_{Bd} + cos\delta_B I_{Bq}\right) \quad (28)$$

These equations can be re-written and after linearization in following matrix format and detail value calculation of K coefficients firstly introduced in [18]:

$$\begin{bmatrix} \Delta\dot{\delta} \\ \Delta\dot{\omega} \\ \Delta\dot{E}'_q \\ \Delta\dot{E}_{fd} \\ \Delta\dot{V}_{DC} \end{bmatrix} = \begin{bmatrix} 0 & \omega_0 I & 0 & 0 & 0 \\ -M^{-1}K_1 & -M^{-1}D & -M^{-1}K_2 & 0 & -M^{-1}K_{pd} \\ -T_{do}^{-1}K_4 & 0 & -T_{do}^{-1}K_3 & T_{do}^{-1} & -T_{do}^{-1}K_{qd} \\ -T_A^{-1}K_5K_A & 0 & -T_A^{-1}K_6K_A & -T_A^{-1} & -T_A^{-1}K_6K_{vd} \\ K_7 & 0 & K_8 & 0 & -K_9 \end{bmatrix} \begin{bmatrix} \Delta\delta \\ \Delta\omega \\ \Delta E'_q \\ \Delta E_{fd} \\ \Delta V_{DC} \end{bmatrix}$$

$$+ \begin{bmatrix} 0 & 0 & 0 & 0 \\ -M^{-1}K_{pe} & -M^{-1}K_{pde} & -M^{-1}K_{pb} & -M^{-1}K_{pdb} \\ -T_{do}^{-1}K_{qe} & -T_{do}^{-1}K_{qde} & -T_{do}^{-1}K_{qb} & -T_{do}^{-1}K_{qdb} \\ -T_A^{-1}K_AK_5 & -T_A^{-1}K_AK_{vde} & -T_A^{-1}K_AK_{vb} & -T_A^{-1}K_AK_{vdb} \\ K_{ce} & K_{cde} & K_{cb} & K_{cdb} \end{bmatrix} \begin{bmatrix} \Delta m_E \\ \Delta\delta_E \\ \Delta m_B \\ \Delta\delta_B \end{bmatrix} \quad (29)$$

As we can see, the above equation is the standard form of the linear system as below:

$$\Delta\dot{X}_g = A_g\Delta X_g + B_g\Delta U \quad (30)$$

This matrix equation is suitable for classical linear control and numerical solving of the system equations as well as analysis such as eigenvalues-related techniques.

V. Modelling of DFIG Connected to Power System

Recently researchers have shown that in a modal study if wind farm is replaced by an equal dynamic DFIG, it will have acceptable result [26]. A comprehensive model of DFIG connected to a power system is similar to Wang' [19] idea that was conducted before FACTS devices were developed [27]. Multi-machine power system linearized model considering DFIG connections (e.g., Figure 2) may be extracted as follows:

$$\frac{d}{dt}\begin{bmatrix} \Delta\delta \\ \Delta\omega \\ \Delta E'_q \\ \Delta E_{fd} \end{bmatrix} = \begin{bmatrix} 0 & \omega_0 I & 0 & 0 \\ -M^{-1}K_1 & -M^{-1}D & -M^{-1}K_2 & 0 \\ -T_{do}^{-1}K_4 & 0 & -T_{do}^{-1}K_3 & T_{do}^{-1} \\ -T_A^{-1}K_5K_A & 0 & -T_A^{-1}K_6K_A & -T_A^{-1} \end{bmatrix} \begin{bmatrix} \Delta\delta \\ \Delta\omega \\ \Delta E'_q \\ \Delta E_{fd} \end{bmatrix} +$$

$$\begin{bmatrix} 0 \\ -M^{-1}k_{PP} \\ -T_{do}^{-1}k_{EP} \\ T_A^{-1}K_Ak_{VP} \end{bmatrix}\Delta P_W + \begin{bmatrix} 0 \\ -M^{-1}k_{PQ} \\ -T_{do}^{-1}k_{EQ} \\ T_A^{-1}K_Ak_{VQ} \end{bmatrix}\Delta Q_W \quad (31)$$

The state vector of the whole grid, $\boldsymbol{X_g}$, in the matrix format while DFIG is connected is as follows:

$$\frac{d}{dt}\Delta \boldsymbol{X}_g = \boldsymbol{A}_g \Delta \boldsymbol{X}_g + \boldsymbol{b}_P \Delta P_w + \boldsymbol{b}_Q \Delta Q_w \quad (32)$$

Where V_W is the bus by which DFIG is connected to power system voltage amplitude that can be represented as below:

$$\Delta V_W = C_g \Delta X_g + d_{g1}\Delta P_W + d_{g2}\Delta Q_W \quad (33)$$

DFIG linearized model can be used in the following format:

$$\frac{d}{dt}\Delta \Psi_{wsd} = K_{wd1}\Delta \Psi_{wsd} + K_{wq1}\Delta \Psi_{wsq} + \cdots + K_{1V}V_w \quad (34)$$

$$\frac{d}{dt}\Delta \Psi_{wsq} = K_{wd2}\Delta \Psi_{wsd} + K_{wq2}\Delta \Psi_{wsq} + \cdots + K_{2V}V_w \quad (35)$$

For any other selected state variable of DFIG:

$$\frac{d}{dt}\Delta x_j = K_{wdj}\Delta \Psi_{wsd} + K_{wqj}\Delta \Psi_{wsq} + \cdots + K_{jV}V_w \quad (36)$$

In matrix format:

$$\frac{d}{dt}\Delta \boldsymbol{X}_w = \boldsymbol{A}_w(p)\Delta \boldsymbol{X}_w + \boldsymbol{b}_w(p)\Delta V_w \quad (37)$$

Output power of DFIG in linear form can be shown as:

$$\begin{bmatrix}\Delta P_w \\ \Delta Q_w\end{bmatrix} = \begin{bmatrix}\boldsymbol{c}_{Pw}^T \\ \boldsymbol{c}_{Qw}^T\end{bmatrix}\Delta \boldsymbol{X}_w + \begin{bmatrix}c_{PV} \\ c_{QV}\end{bmatrix}\Delta V_w \quad (38)$$

We can replace them in Heffron-Philips equations to form matrix format equations containing both power system and DFIG variables:

Here, we have used a more complete model of DFIG so that the state variable vector of DFIG is:

$$\Delta X_w = [\Delta \Psi_{wsd}\ \Delta \Psi_{wsq}\ \Delta \Psi_{wrd}\ \Delta \Psi_{wrq}\ \Delta \omega_{r1}\ \Delta \omega_{r2}\ \Delta \theta_{wr}\ \Delta x_{w1}\ \Delta x_{w2}\ \Delta x_{w3}\ \Delta x_{w4}\ \Delta I_{dcd}\ \Delta I_{dcq}\ \Delta V_{wdc} \Delta x_{w5}\ \Delta x_{w6}\ \Delta x_{w7}]^T \quad (39)$$

Where w index refers to wind (DFIG) parameters, s represents the stator, r is the rotor, d to d axis, q to q axis and dc to dc link. Δx_{w1} to Δx_{w7} are linearized auxiliary variables to consider RSC and GSC dynamics.

Combining Eq. (32), (33), and (38) will form a dynamic equation for both systems as follows:

$$\begin{bmatrix}\Delta \dot{X}_g \\ \Delta \dot{X}_w \\ \Delta \dot{X}_c\end{bmatrix} = A\begin{bmatrix}\Delta X_g \\ \Delta X_w \\ \Delta X_c\end{bmatrix} \quad (40)$$

Where X_c is the state variables related to PIs of DFIG control system.

For the dynamic stability study of the whole system, we should combine Eq. (30) and (40) to reach Eq. (41), which explains multi-machine power system simultaneously contains UPFC and DFIG and we can use it to investigate small signal issues of the whole system.

$$\Delta \dot{X} = A\Delta X + B\Delta U \quad (41)$$

While:

$$\Delta X = \begin{bmatrix}\Delta X_g \\ \Delta X_W \\ \Delta X_c \\ \Delta V_{DC}\end{bmatrix} \quad (42)$$

Dimension of this state vector is *4n+1+17*. n is the number of synchronous generators, 1 state for UPFC and 17 state for DFIG while 7 of them are auxiliary to express PI controllers.

We use Eq. (41) to design control system and, if required, we can do compromising, co-ordination, and optimization using this last overall matrix linear equation.

VI. PARTICLE SWARM OPTIMIZATION ALGORITHM

PSO is a population-based optimization technique to solve optimization problems with constraints. In the PSO system, multiple solutions are candidate and cooperate simultaneously. Each candidate, named a particle, flies in the problem search space looking to land on the optimal position. During the generations, particles adjust their own positions according to their own experience and the experience of particles located in the neighborhood. This algorithm attempts to balance exploitation and exploration by combining global and local search methods, and new velocity and position of each particle will be updated according to the following equations [17]:

$$V_i[k+1] = wV_i[k] + c_1 r_1(pbest_i[k] - X_i[k]) + c_2 r_2(gbest[k] - X_i[k])\ , i = 1,2, \ldots, \quad (42)$$

$$X_i[k+1] = X_i[k] + V_i[k+1] \quad (43)$$

where N is the number of particles, k is the current iteration, w is an inertia weight, r_1 and r_2 are random variables between 0 and 1, c_1 and c_2 are acceleration coefficients, V_i and X_i are the velocity and position of the particle i, respectively, $pbest_i$ are the local best position of particle i, And $gbest_i$ is the global- best position of all particles.

In this study, PSO was used three times; (a) Optimizing J function mentioned above with PSO, the lead-lag controller parameters, T_1 to T_4, and wash-out gain K are adjusted while only UPFC have used in power system. (b); To optimize similar J function (based on Eigen values) to optimize the values of 7 PIs of RSC and GSC of DFIG while only DFIG is connected to the power system. (c) To optimize the same function for the whole system in order to optimize UPFC POD parameters and DFIG PIs parameters simultaneously.

VII. AN INTRODUCTION TO LMI TECHNIQUE APPLICATION

LMIs are matrix inequalities that are linear or affine in a set of matrix variables. They are basically convex constraints, so many optimization problems with convex objective functions and LMI constraints can easily be solved efficiently. Many control problems can be formulated as LMI problems. An LMI has the following form:

$$F(x) = F_0 + \sum_{i=1}^{n} x_i F_i > 0 \quad (44)$$

where $x \in \mathcal{R}^m$ is the vector of decision variables and $F_0, F_1, \ldots, F_n$ are the constant symmetric real matrices, i.e.,

$F_i = F_i^T$,$i = 0, \ldots m$. The inequality symbol in the equation means that $F(x)$ is positive definite, i.e., $u^T F(x) u > 0$ for all nonzero $u \in \mathcal{R}^n$. This matrix inequality is linear in the variables x_i.

In the analysis of the state feedback controller, the objective is to determine a matrix $F \in \mathcal{R}^{m \times n}$ such that all the eigenvalues of the matrix $A + BF \in \mathcal{R}^{n \times n}$ lie in the open left-half of the complex plane. Using Lyapunov theory, it can be shown that this is equivalent to finding a matrix F and a positive definite matrix $P \in \mathcal{R}^{n \times n}$ such that the following inequality holds:

$$(A + BF)^T P + P(A + BF) < 0 \quad (45)$$

or

$$A^T P + PA + F^T B^T P + PBF < 0 \quad (46)$$

Note that the terms with products of F and P are nonlinear or bilinear. Let us multiply either side of the above equation by $Q = P - 1$. This gives:

$$QA^T + AQ + QF^T B^T + BFQ < 0 \quad (47)$$

This is a new matrix inequality in the variables $Q > 0$. But it is nonlinear too. By defining a second new variable$= FQ$, we have:

$$QA^T + AQ + L^T B^T + BL < 0 \quad (48)$$

This gives an LMI feasibility problem in the new variables $Q > 0$ and $L \in \mathcal{R}^{m \times n}$. After solving this LMI, the feedback matrices F and Lyapunov variable P can be recovered from $F = LQ - 1$ and $P = Q - 1$. This shows that by making a change in the variables, we can obtain an LMI from a nonlinear matrix inequality [28]. While LMI solvers are concerned to resolve stability issues, we used LMI to achieve a more acceptable result [29].

VIII. SYSTEM SIMULATION

A. Implementation algorithm

We applied this simulation method to several power systems and we report the results of one of them here. Figure 5 shows the studied power system, which is a 10-machine 39-bus New England network whose data can be found in [30]. For small signal analysis, the sampling time was selected as 0.1 msec, thus the frequency of the two UPFC and DFIG inverters' parameters updating is 10 kHz, which is consistent with the existing switches' speeds. In this study, a PSS was used only for the generator that is installed on the slack bus. We simulated four scenarios: power system without UPFC and without DFIG, power system using UPFC controller only, power system while connected DFIG (wind farm) controller acts, power system while both UPFC and DFIG controllers are simultaneously designed and used.

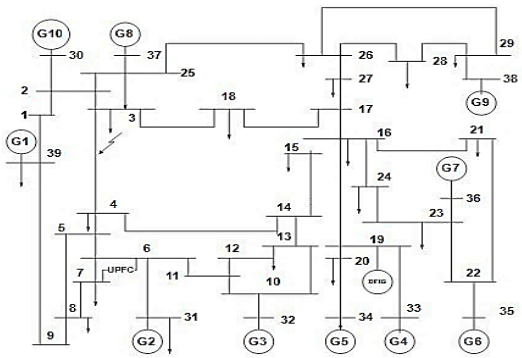
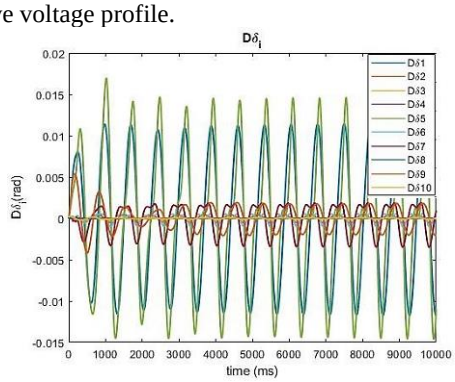


Fig. 5. The New England power system network schematic single line

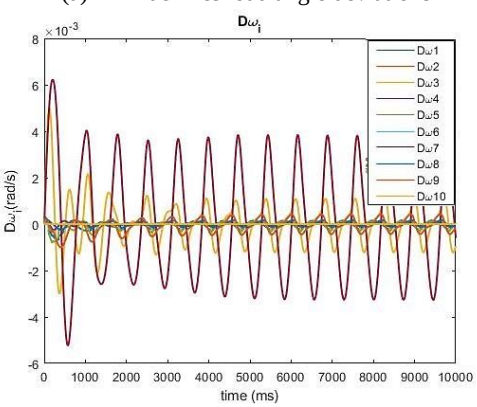
B. Power system simulation results

In this study, MATLAB program was used to simulate the model. Within the load flow solution, the thermal limits of lines capacity are considered. A 3-phase earth fault is applied to the line between bus 3 and 4 and its duration to clear is 0.1 sec which is short enough for small signal analysis. Oscillations are demonstrated by extracting $\Delta\delta$ and $\Delta\omega$ of all machines.

Figure 6 depicts the results while DFIG is not connected and UPFC is not installed. As we can see, the system states are oscillating or have weak damping while UPFC is not installed. (We see in next section that after using UPFC, the system will be more stable after fault clearing.). The results of load flow implementation are used to find UPFC placement to improve voltage profile.



(a) All machines load angle deviations



(b) All machines speed deviations

Fig.6. System oscillations without UPFC and DFIG

C. power system using UPFC controller

The results of load flow implementation are used to find UPFC placement to improve voltage profile and load flow of the power system. Within load flow solution, the thermal limits of lines capacity are considered. After UPFC insertion in the power network, the load flow is executed again. When UPFC is installed between 6 and 7 buses in the system, the active and reactive power loses are reduced. It is also verified that not only the power losses are reduced, the voltage profile of the buses is improved after incorporating UPFC. This simulation is carried out according to flowchart in Figure 7.

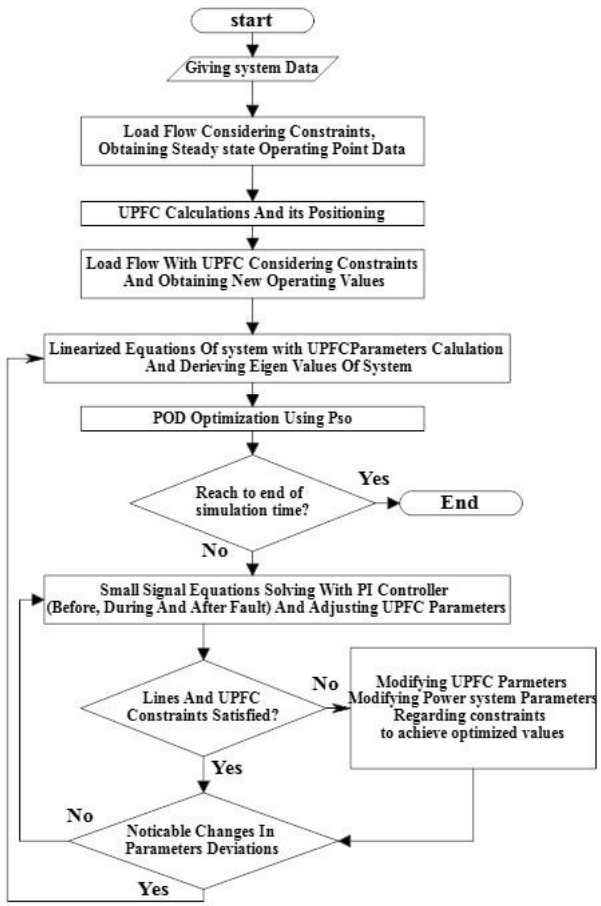


Fig. 7. The flowchart of the simulation of the power system with UPFC installed

For small signal and dynamic stability study, we used UPFC dynamic model and interfacing with power system as described in Section IV. All four basic controllers of UPFC are considered. Eigenvalues and damping ratios of the linearized system are derived and, based on these values, the PSO algorithm is used to optimize damping oscillations controller. Figure 8 demonstrate the eigenvalues of the system with and without UPFC in a complex plane. As we can see, some of eigenvalues have a little more negative real part. Some of critical eigenvalues are shown in Table I.

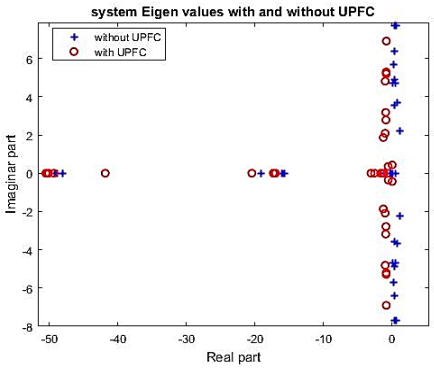


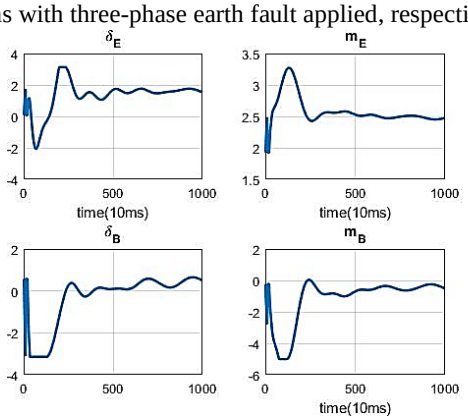
Fig.8. A comparison of the system eigenvalues with and without UPFC

Table I

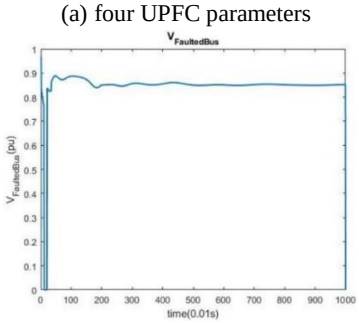
SOME CRITICAL EIGENVALUES BEFORE AND AFTER USING UPFC

Related state	Without UPFC	With UPFC
Machine no. 1 load angle deviation	0.638 + 7.701i	-0.849 - 6.908i
Machine no. 3 load angle deviation	0.292 + 7.707i	-0.871 - 5.203i
Machine no. 1 angular speed deviation	0.286 + 4.887i	-0.948 - 3.181i
Machine no. 3 angular speed deviation	0.478 + 4.702i	-1.287 - 1.866i

To investigate the enhancement of the power system stability by a UPFC, we studied the results and responses of three-phase earth fault scenarios, too. Figures 9(a)-(d) show four UPFC parameters, faulted bus voltage, the variation of all machines load angle variations, and all machines speed variations with three-phase earth fault applied, respectively.

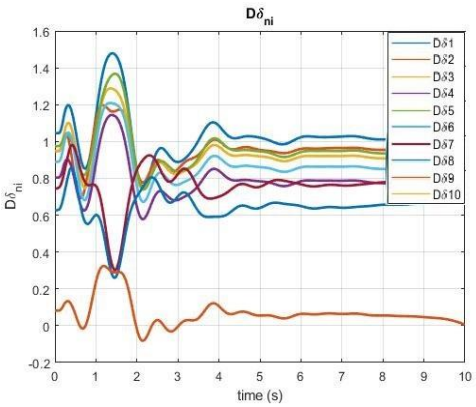


(a) four UPFC parameters

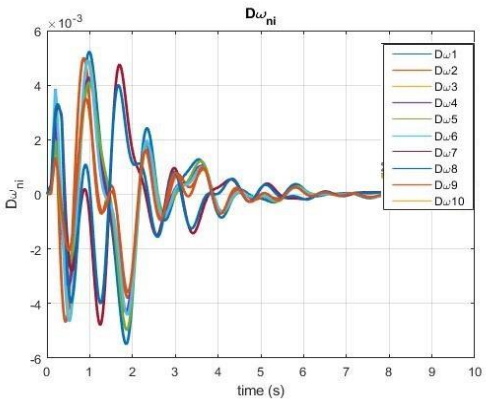


(b) faulted bus voltage

Fig.9 Continued



(c) All machines load angle deviations



(d) All machines speed deviations

Fig.9. Damping performance and effect of UPFC in three-phase earth fault

D. Power system using connected DFIG controller

While DFIG (connected to bus 19 with a short line) controller is used to damp oscillations, we can see that its effect is less than when we used UPFC. But, we found that when we increased the capacity of the wind farm (equal DFIG), its effect on oscillation damping increased too. This simulation was carried out according to the flowchart in Figure 10. Figures 11(a)-(c) depict the variations of all machines load angle, all machines speed variations, and DFIG states as assigned in (39), respectively.

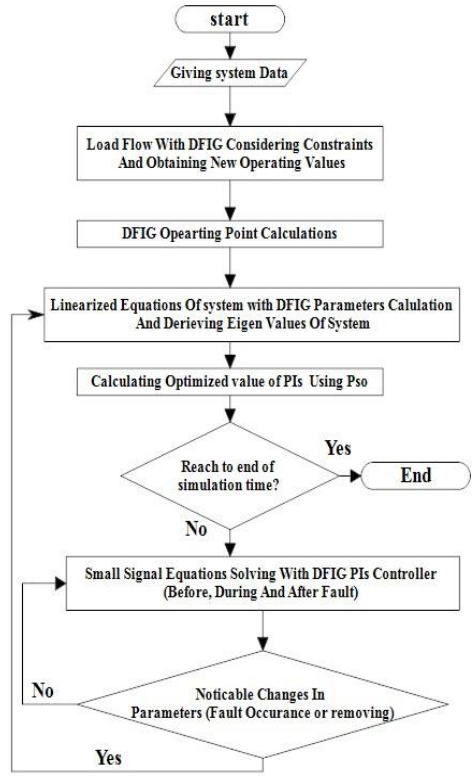
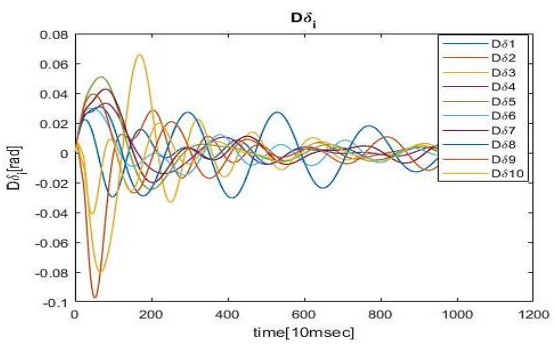
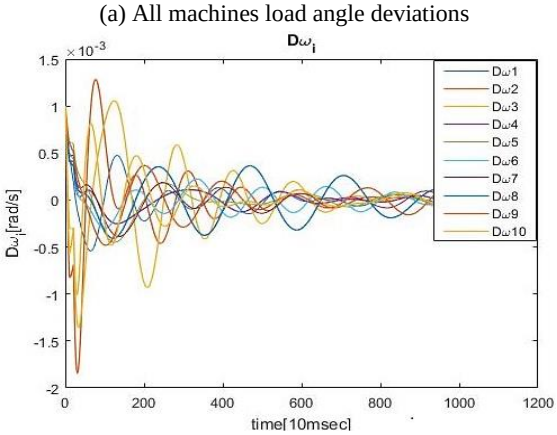


Fig.10. The flowchart of the simulation and power system with DFIG connected

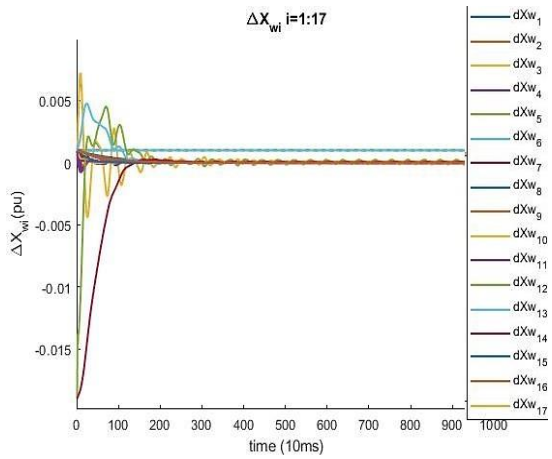


(a) All machines load angle deviations



(b) All machines speed deviations

Fig.11 Continued



(c) DFIG states deviations

Fig.11. Damping effect of DFIG in three phase earth fault

E. Power system using both UPFC and DFIG controller

According to the flowchart in Figure 12, the whole system linearized equation, shown in (42), is used to optimize parameters of both UPFC and DFIG and solve and extract the deviation of the variables. While there are both UPFC and DFIG in power system, and we simultaneously and coordinately designed them in one state matrix, damping effect of them is better than when we used their controller with individual design of them. Figures 13(a)-(c) display the variations of all machines load angle, all machines speed variations, and DFIG states as assigned in equation (39), respectively.

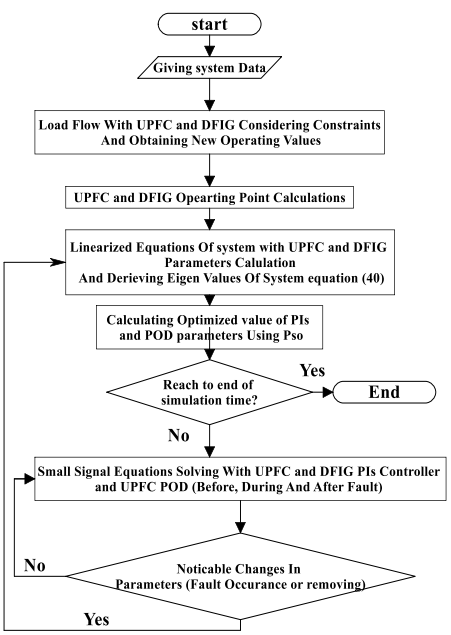
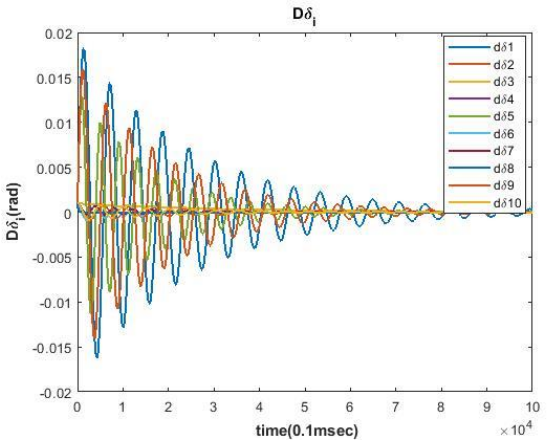
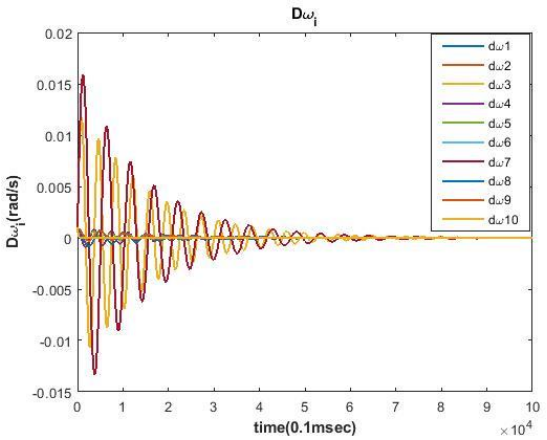


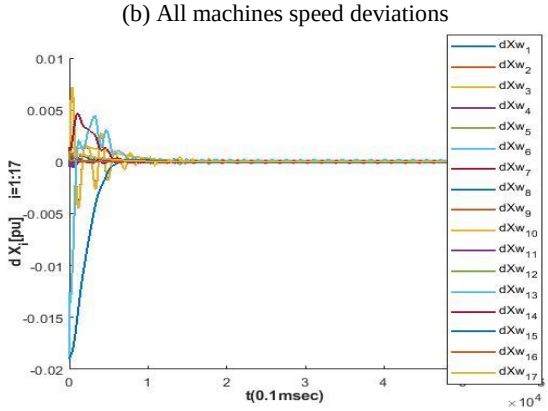
Fig. 12. The flowchart of the simulation and power system with DFIG connected and UPFC installed



(a) All machines load angle deviations



(b) All machines speed deviations



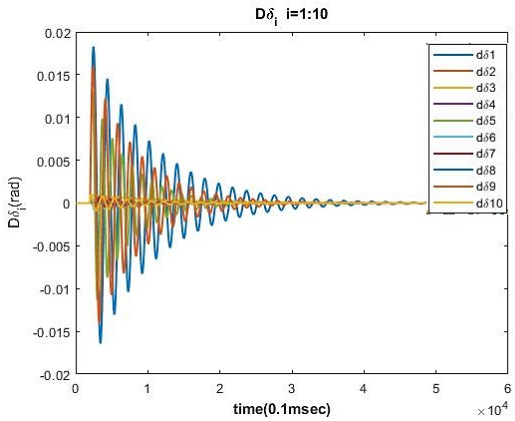
(c) DFIG states variables deviations defined in (39)

Fig.13. Damping effect of both UPFC and DFIG in earth fault while coordinately designed

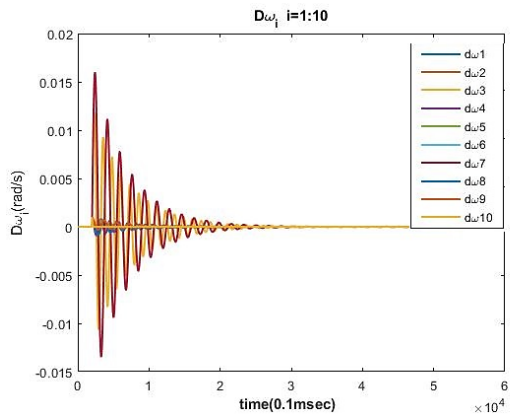
F. Power system using both UPFC and DFIG controller while LMI has used

The system and all situations, described in Section E, were used again to simulate and solve whole system linearized state space model using state feedback control and application of LMI technique, described in Section VI. Figures 14(a)-(c) depict the variation of all machines load angle, all machines speed variations, and DFIG states as assigned in Eq. (39), respectively. While comparing them

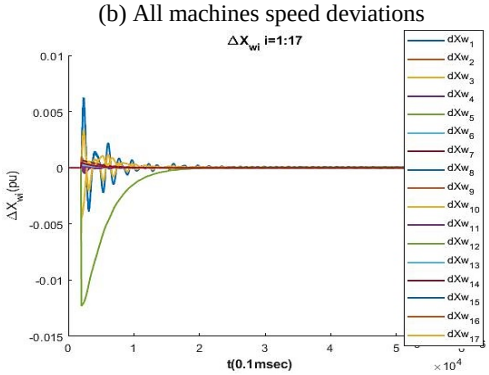
with Figure 13, faster damping and lower overshoots and then more acceptable result is clear. The results of this more complete models' simulation with both UPFC and DFIG controllers by using LMI has more acceptable damping effects versus [1],[2] and [3] which have used only UPFC with classic controller, only DFIG with classic controller, and using LQR, respectively.



(a)All machines load angle deviations



(b) All machines speed deviations



(c) DFIG state variables deviations defined in (39)

Fig. 14. Damping effect of both UPFC and DFIG in earth fault while coordinated designed and LMI used

IX. CONCLUSIONS

In this study, the power system with UPFC and its main and damping controls and its POD here modeled based on the Heffron-Philips model. DFIG small signal modeling was carried out considering its 17 non-mechanical and control state variables. The individual effect of UPFC and DFIG on dynamic stability was also studied. Then, their linearized model was added to the power system model and the modal analysis and dynamic stability of the power system was studied in a 10-machine 39-bus New England multi-machine power system. The results show that UPFC can noticeably improve dynamic stability of the whole power system. The control of DFIG in power system helps the system to improve the dynamic stability of DFIG and the power system. While there are both of these two devices in the multi-machine power system, by coordinating and making some optimization in UPFC parameters and controllers and optimized adjustment in DFIG controllers, the dynamic stability of DFIG and the power system can be improved. The result is better when LMI is used versus when only classic described controllers are used. When using LMI, after 4 seconds oscillations are acceptably damped while before using LMI, near 9 seconds was required to damp oscillations acceptably.

APPENDIX

A: UPFC used Data:

In 39-bus New England network: UPFC Rating=190 MW=1.9 pu, xE= 0.0725 pu, xB=0.0725 pu, C=1 pu, Sb=100MW.

B: DFIG used Data:

Mw=3.4, Dwm=0, Rwr=0.0007, Kwm=3.95,
Jwr1=8, Jwr2=8, Dwr1=0.0, Dwr2=0.0,
Xws=0.0878, Xwr=0.0373, Xwm=1.3246, Xwr3=0.05,
Xwf=0.05, sw0=-0.01, Cw=13.29, Rws=0, DFIG rating power=56MW=0.56 pu

REFERENCES

[1] A. Ziaei , R. Ghazi , R. Zeinali davarani, "Linear Modal Analysis of Doubly-Fed Induction Generator (DFIG) Torsional Interaction: Effect of DFIG Controllers and System Parameters", *Advances in Electrical and Electronic Engineering*, pp. 388-401, 2018.

[2] M. Ravindrababu, G. Saraswathi, K.R. Sudha, "Design of UPFC-PSS using Firefly Algorithm for Stability Improvement of Multi Machine System under Contingency", *Majlesi Journal of Electrical Engineering* , vol. 13, No. 2, pp. 21-39, June 2019.

[3] B. K. Dubey, N.K. Singh, "Multimachine Power System Stability Enhancement with UPFC Using Linear QUADRATIC Regulator Techniques", *International Journal of Advanced Research in Engineering and Technology (IJARET)*, vol. 11, Issue 4, pp. 219-229, April 2020.

[4] N. Nahak, R. K. Mallick, S. P. Muni, "Stability Enhancement of Multi machine System by Improved GWO Optimized UPFC based controller", *International Journal of Pure and Applied Mathematics*, vol. 114 no. 9, pp. 63-72, 2017.

[5] S.Q. Bu, X. Zhang, J.B. Zhu, X. Liu, "Comparison analysis on damping mechanisms of power systems with induction generator based wind power generation", *Electrical Power and Energy Systems*, pp. 250–261, 2018.

[6] Y. Mohammed, R. Alharbi, Application of Unified Power Flow Controller to Improve the Performance of Wind Energy Conversion System, Phd thesis, Department of Electrical and Computer Engineering, Curtin University, March 2016.

[7] S. Vig, B. S. Surjan, Advances in Smart Grid and Renewable Energy , in chapter: Analysis of UPFC Controller Connected with Multiple Wind Turbines by Using IEEE Bus System, Springer ,Singapore, 2021.

[8] P. Khandelwal, B. Modi, S. S. Sharma, "DFIG based WECS Connected Power System Using UPFC for Improvement of Stability", International Journal of Research and Scientific Innovation, vol. I, Issue IV, pp. 10-15, September 2014.

[9] A. Ganesan, R. Rajamoort, "Modeling of FUZZY Controlled UPFC for LVRT Improvement in DFIG Based Grid Connected Wind Farm", *Journal of Electronic Design Engineering*, vol. 5 Issue 1, pp. 29-38, MAT Journals 2019.

[10] M. Ferdosian, H. Abdi, A. Bazaei , "Improving the Wind Energy Conversion System Dynamics during Fault Ride through: UPFC versus STATCOM", *IEEE 2015 IEEE International Conference on Industrial Technology (ICIT)*, pp. 2721-2726, 2015.

[11] Y. M. Alharbi, A. M. S.Yunus, A. Abu-Siada, "Application of UPFC to Improve the FRT Capability of Wind Turbine Generator", *International Journal of Electrical Energy*, vol. 1, No. 4, pp. 188-193, December 2013.

[12] Nidhi Vaishnava Amit Verma , Performance Analysis of DFIG based Wind Turbine System using FACTS Devices , *International Journal of Science Technology & Engineering*, Volume 4, Issue 1, pp. 178-183, July 2017.

[13] P. K. Dash, R. K. Patnaik, S. P. Mishra, Adaptive fractional integral terminal sliding mode power control of UPFC in DFIG wind farm penetrated multimachine power system, *Protection and Control of Modern Power* Systems (2018) 3:8, pp. 1-14,2018 https://doi.org/10.1186/s41601-018-0079-z.

[14] D. E. Tourqui, M. Benakcha, T. Allaoui, "Improving the Electrical Stability by Wind Turbine and UPFC, Improving the Electrical Stability by Wind Turbine and UPFC", *Artificial Intelligence in Renewable Energetic Systems*, Springer International Publishing AG 2018. https://doi.org/10.1007/978-3-319-73192-6_13.

[15] H. R. Koofigar, G. Isazadeh, "Optimal robust stabilizer design based on UPFC for interconnected power systems considering time delay", Archives of Electrical Engineering vol. 66(3), pp. 459-474, 2017.

[16] H. Zhang, J. Hao, C. Wu, Y. Li, A. Sahab, "A novel LMI-based robust adaptive model predictive control for DFIG-based wind energy conversion system", system science & control engineering, vol. 7, pp. 311-320, 2019.

[17] Y. Shi, R. Eberhart, "A modified particle swarm optimizer", *IEEE international conference on evolutionary computation proceedings*, Anchorage, AK, USA, pp. 69–73, 1998.

[18] A. Nabavi-Niaki, M.R. Iravani, "Steady-state and dynamic models of unified power flow controller for power system studies", *IEEE Transactions on Power System*, vol. 11, no. 4, pp. 1937-1950, 1996.

[19] H.F. Wang, "A unified model for the analysis of FACTS devices in damping power system oscillations –Part III: unified power flow controller', *IEEE Transaction on Power Delivery*, vol. 15, no. 3, pp. 978–983, 2000.

[20] H.F. Wang, M. Jazaeri, Y.J. Cao, ¨Analysis of control conflict between UPFC multiple control functions and their interaction indicator", *International Journal of Control, Automation and Systems*, vol. 3, no. 2(special edition), pp. 315-321, 2005.

[21] K. Madhuri, M.V. Srikant, "Modeling and analysis of power flow controller in the presence of power system stabilizer for a multi-machine system", *International Journal of Engineering Research & Technology (IJERT)*, vol. 1, no. 6, pp. 1-7, 2012.

[22] M. Eslami, H. Shareef, M.R. Taha, M. Khajezadeh," Adaptive particle swarm optimization for simultaneous design of UPFC damping controllers", *ELSEVIER Electrical Power and Energy Systems*, vol. 57, pp. 116-128, 2014.

[23] J. Fletcher, J. Yang, "Introduction to the Doubly-Fed Induction Generator for Wind Power Applications", *D. A. Ng, Ed.*, InTech, pp. 259-279, 2010.

[24] H. *Jiang*, H. Liu, L. Wu, Y. Li, "*Comparisons* on State Space Models of Doubly Fed Induction Generators (*DFIG*) for Power System Research", *State Grid Jibei Electric Power Research Institute. Beijing, China. IEEE PES Asia-Pacific Power and Energy Conference* - Xi'an – China, 2016. DOI: 10.1109/APPEEC.2016.7779624.

[25] P. Kundur, "Power System Stability and Control", Electric Power Research Institute, Power System Engineering Series, McGraw-Hill, New York, 1994.

[26] W. Du, X. Chen, H.F. Wang, "Impact of dynamic interactions introduced by the DFIGs on power system electromechanical oscillation modes", *IEEE, 0885-8950 (c)*, 2016.

[27] W. Du, J. Bi, C. Ly, T. Littler, "Damping torque analysis of power systems with DFIGs for wind power generation", *IET Proceedings on Renewable Power Generation*, on-line early view, 2016.

[28] Z. Jian**,** S**.** Akshya**,** N**.S.** Kiong, Robust Observer based Fault Diagnosis for nonlinear systems using MATLAB, springer,



Masoud Maleki rizi received his B.Sc. degree in Electrical Engineering from Tabriz University, Tabriz, Iran in 1997 and his M.Sc. degree in Electrical Engineering from Isfahan University of Technology, Isfahan, Iran in 2001. He is currently a Ph.D. candidate in Electrical Engineering at Shahrekord University, shahrekord, Iran. His research interests are power system dynamic stability, FACTS devices impact on power system stability, power system control and stability optimization, and renewable energy systems.



Saeed Abazari received his B.Sc. degree in electrical engineering from Isfahan University of Technology, Isfahan, Iran, in 1989, the M.Sc. degree from Ferdowsi University, Mashhad, Iran, in 1992 and the Ph.D. degree from Sharif University of Technology, Tehran, Iran, in 2002. Currently, He is a Professor of the Electrical Engineering Department at the Shahrekord University, Shahrekord, Iran. His research interests are electric power distribution system, smart grid, power system operation and control and FACTS controllers.



Nima Mahdian Dehkordi received the M.Sc. and Ph.D. degrees from Sharif University of Technology, Tehran, Iran, in 2012 and 2016, respectively, both in electrical engineering. He joined the the Department of Electrical Engineering, Science and Research Branch, Islamic Azad University, Tehran, Iran, in2017, where he is currently an Assistant Professor. His research interests include control systems, applications of control theory in power electronics, microgrid control, distributed and cooperative control, internet of things, nonlinear control, and network control.

IECO

This page intentionally left blank.